

## Modeling and Optimal Centralized Control of a Large-Size Robotic Population

Dejan Milutinović and Pedro Lima

**Abstract**—This paper describes an approach to the modeling and control of multiagent populations composed of a large number of agents. The complexity of population modeling is avoided by assuming a stochastic approach, under which the agent distribution over the state space is modeled. The dynamics of the state probability density functions is determined, and a control problem of maximizing the probability of robotic presence in a given region is introduced. The Minimum Principle for the optimal control of partial differential equations is exploited to solve this problem, and it is applied to the mission control of a simulated large robotic population.

**Index Terms**—Hybrid automata, multirobot systems, optimal control.

### I. INTRODUCTION

Multiagent systems (MAS), concerning both virtual [1], [2] and real (robotic) [3], [4] agent populations, are currently a subject of major interest in the literature. One of the most relevant topics in MAS is the modeling of large-size agent populations.

Deterministic modeling and control approaches have been used both for large-size [5] and small-size [6] robot formations. On the other hand, the task allocation and task performance of groups of robots were modeled under a probabilistic framework in [7]–[9].

In this paper, we are proposing a modeling approach which considers not only the probabilistic description of task allocation, but also the distribution of the population over the operating space. This is based on our recent results [10] on the mathematical modeling of biological systems [11]. In fact, our work was originally developed for modeling cell interaction [10], but we found that such an approach also provides results of potential interest for the MAS community [10], [12].

We introduce a model of robotic population, which is based on a Stochastic Hybrid Automaton model [13]. Using statistical physics [14] in this framework, the population state is defined by the probability density function (PDF). Our model is the system of partial differential equations (PDEs) that describes the evolution of the population state. This evolution depends on the population parameters, and some of them can be considered as control inputs. Therefore, based on the proposed modeling approach, we also derive control theory principles for large-scale robotic populations.

The main motivation of our approach is to provide fundamental principles of modeling and control for large-size populations, providing math-based tools for the analysis and control design from specifications. We assume that the robotic population can execute the primitive tasks driven by individual robot controllers and local information. For example, each primitive task may correspond to one motion primitive. The population is governed by a centralized controller, which sends commands for task execution, task cancellation, or task switching. In

Manuscript received January 5, 2006. This paper was recommended for publication by Associate Editor D. Fox and Editor H. Arai upon evaluation of the reviewers' comments. This work was supported by the Portuguese Fundação para a Ciência e a Tecnologia under Grant SHFR/2960/2000. This paper was presented in part at the IEEE International Conference on Advanced Robotics, Coimbra, Portugal, 2003.

D. Milutinović was with the Institute for Systems and Robotics, Instituto Superior Técnico, 1049-001 Lisbon, Portugal. He is now with the Department of Theoretical Biology, Utrecht University, 3584CH Utrecht, The Netherlands.

P. Lima is with the Institute for Systems and Robotics, Instituto Superior Técnico, 1049-001 Lisbon, Portugal (e-mail: pal@isr.ist.utl.pt).

Digital Object Identifier 10.1109/TRO.2006.882941

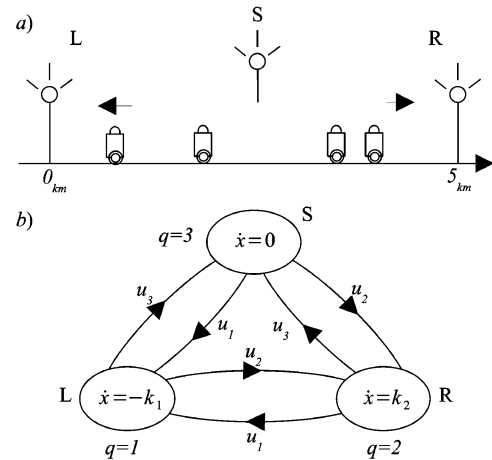


Fig. 1. (a) Robotic population controlled by three signal sources. (b) Robotic population microagent model [10].

such a way, the population is controllable as a single conventional general-purpose robot. The centralized control strategy for a large-size robotic population must take into account the uncertainty of each individual robot reaction, due to communication problems, local characteristics of the surrounding environment, etc. This uncertainty is included in our PDE model.

The proposed centralized controller is based on the Pontryagin–Hamiltonian optimal control theory for PDEs [15], and provides the control of the population space distribution shape. However, as in classical optimal control [16], it is an open-loop controller and there is no warranty that the control can be expressed analytically. For the numerical computation of optimal control, discrete approximations in time and space are necessary.

### II. MODELING AND CONTROL OF THE POPULATION

We support the description of our method by a motivating scenario. The scenario, which introduces a class of optimal control problems formulated in this paper, assumes a robotic population with a *large number of small* mobile robots. The term *small* is used here to underline that the robot dimensions are significantly smaller than the dimensions of the region where the robots are operating. We also assume that the robotic population is sparse, and therefore, no local interactions among robots are considered.

Several robots are initially distributed over the operating space and controlled by signal sources from aerial robots (Fig. 1). In this scenario, each robot in the population moves left and right in the direction of an active signal source, or stops when the stop signal is active. In this case, the three vector fields directing the robots left, right, and stop are  $f_1(x) = -k_1$ ,  $f_2(x) = k_2$ , and  $f_3(x) = 0$ , respectively. Thus, each robot within the population can be in one of the three possible discrete states  $q = 1, 2, 3$ . The control objective is to maximize the robots' presence in a desired region of the operating space along the  $x$  axis.

The land robot population is steered by active signal sources generated by the aerial robots. However, not all the robots will react at the same time and change their motion at once. This happens because the population is composed of a large number of independent robots. The uncertainty affecting the robot reaction to the sent command is included in our modeling approach. This uncertainty can result from *physical constraints to the robot*, such as existence of physical barriers between the specific robot and the signal source. The other reasons for the uncertainty can result from the *limitation of robot resources*. For example, a

robot endowed with solar-light rechargeable batteries might rest till its batteries have been fully recharged, and would not react to commands meanwhile. To follow the complete dynamics of the population, we need to model the reaction and motion of each robot. However, in order to apply optimal control theory, a relationship between the robotic population spreading over the operating region and the population control signals must be established in such a way that mathematical analysis is possible. This fact motivated our general approach to the modeling and control of a multiagent population.

Since the individual robot reaction to the command depends on many *uncertain factors*, we can model this reaction by stochastic transitions between discrete states, each of them representing a particular robot behavior. In our scenario, each individual robot can be modeled by the hybrid automaton model, presented in Fig. 1(b), which includes stochastic transitions between the discrete states  $q$ .

The mission control in this case concerns the control of the stochastic transition rates  $u_i, i = 1, 2, 3$ , in such a way that the robotic presence in a desired region along the axis  $x$ , is maximized. The mission-control problem we are considering here is an open-loop control problem. Its closed-loop version would take into account the environment changes over the space as the robots move, and potential changes in the robotic population, such as failures and commands not executed properly. Therefore, the closed-loop control would lead to different  $u_i$  control requirements.

The robotic scenario introduced here is the simplified version of possible real-world examples. One major simplification is that communication among the robots is not considered. However, this helps us in achieving a mathematical description suitable to model large-size robotic populations, which can be exploited for the model-based control design. This is a paramount idea of this paper, and the robotic scenario we are considering is along this line of thought.

The state of the individual robot is composed of a discrete and a continuous component. Therefore, the state PDF of the model presented in Fig. 1(b) is given by the vector  $\rho(x, t) = [\rho_1(x, t)\rho_2(x, t)\rho_3(x, t)]'$ . Each  $\rho_i, i = 1, 2, 3$  describes the PDF component corresponding to the discrete state  $i$ . The modeling we are applying here is detailed in [10].

The following system of equations describes the evolution of the robotic population state PDF:

$$\frac{\partial \rho(x, t)}{\partial t} = F(u)\rho(x, t) = (F_u(u(t)) + F_\partial)\rho(x, t) \quad (1)$$

with

$$F_u(u) = \begin{bmatrix} -u_2 - u_3 & u_1 & u_1 \\ u_2 & -u_1 - u_3 & u_2 \\ u_3 & u_3 & -u_1 - u_2 \end{bmatrix} \quad (2)$$

$$F_\partial = \text{diag} \left( k_1 \frac{\partial}{\partial x}, -k_2 \frac{\partial}{\partial x}, 0 \right)$$

where  $u(t) = [u_1(t)u_2(t)u_3(t)]'$  with  $'$  denoting the vector transposition, and the symbol  $t$  in  $u(t)$  is omitted in (2). The operator  $F(u)$  is composed of the two components,  $F_u$  and  $F_\partial$ , corresponding to the discrete state transitions and the motion of the robots, respectively [10]. This system of PDEs is derived directly from the model shown in Fig. 1(b), and describes the dynamics of the robotic population without local interactions among the robots, or between the robots and the environment.

The probabilistic approach we are using here is of fundamental importance to reach a mathematically tractable approach to the *spatio-temporal* modeling of large-size robotic populations. The validity of the model can be evaluated and the model accuracy will be certainly dependent on the robotic population size and on the type of the operating environment uncertainties. Instead of going into modeling details,

we are more interested in the fundamental question of how this type of model can be exploited for control.

If we consider that the robotic population parameters depend on the control vector  $u(t)$ , then the optimal control problem is to find a control  $u(t)$  such that the following cost function is maximal:

$$J(u) = \int_X w'(x)\rho(x, u; T)dx \quad (3)$$

where  $w(x) = [w_1(x)w_2(x)w_3(x)]'$  is a vector of weighting functions,  $T$  is the time duration of the mission, and  $\rho_i, i = 1, 2, 3$  depend on  $u$ . In general,  $u$  is a vector of the population parameters that may be set externally by appropriate commands sent to the population. Here we consider the control problem where  $u$  is a time-dependent vector composed of transition rates having the values between 0 and the maximal value  $u_{\max}$ , i.e., the set of admissible controls for  $u(t) = [u_1(t)u_2(t)u_3(t)]'$  is  $U_{\text{ad}} = \{[0, u_{\max}] \times [0, u_{\max}] \times [0, u_{\max}]\}$ . Transitions are events dependent on correct command reception and conditions for command execution. Therefore, transition rates depend on the frequency of commands resending and environment characteristics. To specify completely the solution of (1), the initial and boundary conditions must be defined, and we will do that in the next section.

The optimal control problem is to determine the optimal control  $u = u^*$  which *maximizes* the criterion (3). This problem can be considered as a special case of a more general optimal-control problem of the *evolution equation* [15]. Under the condition that the operator  $F(u)$  is bounded, i.e.,  $\|F(u(t))\| < \infty$ , the minimum principle for PDEs can be applied [15]. The Hamiltonian is

$$H(\rho(x, t), u, t) = \langle \pi(x, t), F(u)\rho(x, t) \rangle \quad (4)$$

where brackets  $\langle \cdot, \cdot \rangle$  denote the scalar product of function vectors defined as

$$\langle p(x), q(x) \rangle = \int_X p'(x)q(x)dx. \quad (5)$$

The function vector  $\pi(x, t)$  is the so-called adjoint state, and satisfies

$$\frac{\partial \pi(x, t)}{\partial t} = -F'(u^*)\pi(x, t) \quad (6)$$

$$\pi(x, T) = -w(x).$$

According to the minimum principle for PDEs [15], the optimal control  $u^*(t)$  satisfies

$$u^*(t) = \arg \min_{u \in U_{\text{ad}}} H(\rho^*(x, t), u(t), t). \quad (7)$$

In words, for the optimal state trajectory  $\rho^*(x, t)$ , the optimal control *minimizes* the Hamiltonian at each time point.

### III. APPLICATION TO A ROBOTIC POPULATION

The initial robotic population state PDF is given by the initial PDF of robots moving left, moving right, and not moving along the  $x$  axis,  $\rho_1(x, 0) = 0, \rho_2(x, 0) = 0$  and

$$\rho_3(x, 0) = \begin{cases} \frac{1}{\sqrt{0.02\pi}} \exp\left(-\frac{(x-2.5)^2}{0.02}\right), & 2 < x < 3 \\ 0, & \text{otherwise} \end{cases} \quad (8)$$

respectively. The duration of the robotic mission is  $T = 3h$ , and the weighting function  $w_3(x)$  is

$$w_3(x) = \begin{cases} \frac{1}{\sqrt{0.01}} \exp\left(-\frac{(x-1.75)^2}{0.01}\right), & 1.25 < x < 2.25 \\ 0, & \text{otherwise} \end{cases}. \quad (9)$$

The optimal-control problem for the robotic mission is given by the cost function

$$J = \int_X \underbrace{[0 \ 0 \ w_3(x)]}_{w'} \rho(x, T). \quad (10)$$

The motivation for the weighting function  $w_3$  choice is to compute control that will move the center of the robotic distribution from 2.5 to 1.75, and make the distribution slightly sharper.

To show that the operator  $F(u)$  is bounded and to apply the *minimum principle*, we should first define a space of the state  $\rho$  and costate  $\pi$  variables. We will assume that the solutions  $\rho, \pi$  of (1) and (6), respectively, are from the same space of functions  $E$  that satisfies

$$\rho, \pi \in E \quad (11)$$

$$\rho, \pi : X \rightarrow L^2 \times L^2, \partial X \rightarrow 0$$

$$d(\rho_i^2), d(\pi_i^2) : \text{Lebesgue integrable}, \quad i = 1, 2. \quad (12)$$

The symbol  $L^2$  stands for the set of Lebesgue measurable functions [17],  $\partial X$  for the boundary of the function domain  $X$ , and the symbol  $d$  for differentiation. Therefore, we will assume that  $X = [0, 5]$  and the boundary conditions

$$\rho(0, t) = \rho(5, t) = \pi(0, t) = \pi(5, t) = 0, t \in [0, T]. \quad (13)$$

The weighting function  $w_3(x)$ , and initial PDFs  $\rho_1(x, 0)$  and  $\rho_3(x, 0)$  are presented in Figs. 4 and 5. The *nonzero* intervals of  $w_3(x)$  and  $\rho_3(x, 0)$  ensure that the boundary conditions (13) are satisfied, i.e., that the population will not have time to reach the boundary of  $X$ .

Using the scalar product defined by (5), the space  $E$  of the functions  $\rho$  is a Hilbert space [17] with the norm

$$\|\rho\| = (\langle \rho, \rho \rangle)^{\frac{1}{2}}.$$

Therefore, we have

$$\|F(u)\rho\| = \langle F(u)\rho, F(u)\rho \rangle$$

and the operator norm

$$\|F(u)\| = \max_{\|\rho\| \leq 1} \|F(u)\rho\|.$$

To show that the operator  $F(u)$  is bounded, we use a triangular inequality

$$\|F(u)\| = \|F_u(u) + F_\partial\| \leq \|F_u(u)\| + \|F_\partial\|.$$

The linear operator  $F_\partial$  is symmetric and we will exploit this to find its norm as

$$\|F_\partial\| = \max_{\|\rho\| \leq 1} |\langle \rho, F_\partial \rho \rangle|.$$

However, applying the definition of the scalar product (5), and by virtue of the space  $E$  property (12), we have

$$|\langle \rho, F_\partial \rho \rangle| = 0 \quad \forall \rho \Rightarrow \|F_\partial\| = 0.$$

$F_u(u)$  is a matrix with finite real coefficients corresponding to the values in the admissible set of controls  $U_{\text{ad}}$ . For any choice of admissible control values, there exists a maximal singular value  $\sigma_{\text{max}}(F_u(u))$ , which is a finite number. Therefore, we can draw the conclusion that the operator  $F(u)$  is bounded, i.e.,

$$\|F(u)\| \leq \max_{u_1, u_2, u_3 \in U_{\text{ad}}} \|F_u(u)\|.$$

Therefore, we can exploit (7) to find the optimal control. The system of equations which describes the evolution of the costate variables is (6) with

$$\pi_1(x, T) = \pi_2(x, T) = 0, \pi_3(x, T) = -w_3(x)$$

and the optimal control  $u^*(t) = [u_1^*(t) \ u_2^*(t) \ u_3^*(t)]'$  satisfies (7), which is equivalent to [10]

$$u^*(t) = \arg \min_{u_1, u_2, u_3 \in U_{\text{ad}}} [u_1 I_1(t) + u_2 I_2(t) + u_3 I_3(t)] \quad (14)$$

where  $I_1(t), I_2(t), I_3(t)$  are functions depending on  $\rho^*(t)$  and  $\pi^*(t)$ . If we can compute  $I_1(t), I_2(t)$  and  $I_3(t)$ , then the optimal control  $u^*(t)$  will be defined as follows:

$$u_i^* = \begin{cases} 0, & I_i(t) > 0 \\ u_{\text{max}}, & I_i(t) < 0 \\ u_i^* \in U_{\text{ad}}, & I_i(t) = 0 \end{cases} \quad i = 1, 2, 3.$$

To compute the optimal control using this expression, we should prove that either  $I_i(t) \neq 0 \forall t \in [0, T]$ , or that  $I_i(t) = 0$  only for a discrete set of time instants  $t_k$ . In the other cases, we can conclude that (14) is still valid, but cannot help us to calculate the control  $u_i^*(t)$  because for  $I_i(t) = 0$ , the control can take any value from the admissible set  $U_{\text{ad}}$ . This is the “singular control” problem [16]. In that case, some further structural properties of PDE systems (1) and (6) must be examined. To avoid the “singular control” problem in our example, we can modify the cost function (10), adding the term which depends on the control  $u$  and is penalized by the parameter  $\varepsilon > 0$ . This results in

$$J^\varepsilon = \int_X w' \rho(x, T) - \varepsilon \int_0^T u_1^2(t) + u_2^2(t) + u_3^2(t) dt. \quad (15)$$

Using a small  $\varepsilon$ , we have  $J \approx J^\varepsilon$ . Applying the minimum principle, the Hamiltonian  $H^\varepsilon$ , corresponding to the problem with the cost function  $J^\varepsilon$ , is [10]

$$H^\varepsilon(t) = H(t) + \varepsilon (u_1^2(t) + u_2^2(t) + u_3^2(t)) \quad (16)$$

and the optimal control is defined as follows:

$$u_i^* = \begin{cases} 0, & -\frac{I_i(t)}{2\varepsilon} > 0 \\ u_{\text{max}}, & -\frac{I_i(t)}{2\varepsilon} < u_{\text{max}} \\ -\frac{I_i(t)}{2\varepsilon}, & \text{elsewhere} \end{cases} \quad i = 1, 2, 3 \quad (17)$$

In this case, the problem of singular control does not exist.

Avoiding the “singular control” problem in this way results in an iterative numerical algorithm for computing the optimal control, proposed in the next section, that will not indefinitely stop at the points where  $I_i(t) = 0$ , without the warranty that the computed control is optimal. The price paid is that we are not solving the original optimal-control problem, but the control problem with the cost function  $J^\varepsilon$ .

The numerical algorithm used in this paper is based on the nonlinear conjugate gradient method [18], which is proposed as an efficient gradient-based method for Hamiltonian minimization in optimal control of ordinary differential equations (ODEs) [18]. To compute the optimal control, we are dealing with the discrete time approximation of the control. This type of control is so-called numerical optimal control [19]. Shortly, given the time range  $[0, T]$ , and discretization steps in space  $\Delta X$  and time  $\Delta T$ , the algorithm is composed of the following steps.

- Step 1) Calculate the discrete approximation  $\hat{\rho}(x, t)$  of the time-forward solution  $\rho(x, t)$ , using the discretized version of (1) and the control  $\hat{u}^j(k)$  in the iteration  $j$ , given the initial condition  $\rho(x, 0)$ .
- Step 2) Calculate the discrete approximation  $\hat{\pi}(x, t)$  of the time-backward solution  $\pi(x, t)$ , using the discretized (6) and  $\hat{u}^j(k)$ , given the terminal condition  $\pi(x, T) = -w(x)$ .
- Step 3) Increase the iteration counter  $j$  by 1 and go to Step 4, or stop the algorithm if the cost function  $J^\varepsilon(j)$  reaches the maximum.
- Step 4) For each  $k$ , calculate the control by the nonlinear conjugate gradient update rule [18].

Since the discretization steps, initial condition, and weighting function are fixed, the result of the algorithm will depend on the free parameter  $\varepsilon$  and the initial guess  $\hat{u}^1(k)$ .

The chosen value for  $\varepsilon$  depends on how close to  $J$  we want  $J^\varepsilon$  to be. The smaller the  $\varepsilon$ , the closer  $J^\varepsilon$  should be to  $J$ . However,  $\varepsilon$  can not be infinitely small, because the algorithm convergence may be influenced when the minimization problem is close to the original problem with the “singular control.” For decimal precision of  $d_p$ , the term which penalizes control in  $J^\varepsilon$  must be smaller than  $10^{-d_p}$ . Since we know the maximal values of control  $u_{\max}$ , this can be expressed by

$$10^{-d_p} > J - J^\varepsilon = \varepsilon \int_0^T \sum_{i=1}^3 u_{\max}^2 dt \approx 3T u_{\max}^2 \varepsilon \quad (18)$$

which means that

$$\varepsilon < \frac{10^{-d_p}}{3T u_{\max}^2}. \quad (19)$$

In the original PDE, the function vector  $\rho(x, t)$  is considered as a state vector of the population at time  $t$ . In the discretized version, the state vector is approximated by  $\hat{\rho}$ , a finite-dimension state vector whose dimension is given by

$$\dim(\hat{\rho}) = NM^D \quad (20)$$

where  $N$  is the number of discrete states, in our example  $N = 3$ ,  $M$  is the number of finite elements used for the space discretization, and  $D$  is the dimensionality of the operating space. The dimension (20) can be used as a measure of the computational complexity of the proposed algorithm. The complexity of the algorithm increases linearly with the number of discrete states, and to the power  $D$ , regarding the number of finite elements  $M$ . The only free parameter to “control” the complexity is the number of the finite elements. However, during the algorithm development, we noticed that a small number of finite elements leads to a poor approximation of the integrals for computing the Hamiltonian.

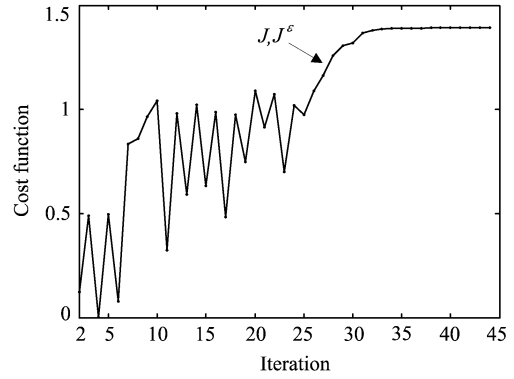


Fig. 2. Cost functions.  $J^\varepsilon$ : the cost function introduced to avoid the singular control problem;  $\varepsilon = 10^{-7}$ ,  $J$ : the original control problem cost function;  $u_i \in [0, 2]$ ,  $i = 1, 2, 3$ . Graphs of  $J^\varepsilon$  and  $J$  are overlapped.

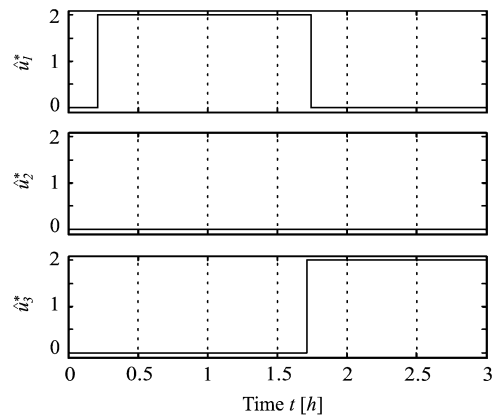


Fig. 3. Components of control  $\hat{u}^* = [\hat{u}_1^* \hat{u}_2^* \hat{u}_3^*]'$  computed after 44 iterations. The control is computed for the cost function  $J^\varepsilon$ ,  $\varepsilon = 10^{-7}$ ,  $\Delta T = 0.03h$ ,  $T = 3h$ ,  $u_i \in [0, 2]$ ,  $i = 1, 2, 3$ .

Consequently, our algorithm can converge to a *nonoptimal* control solution.

The major difficulty in extending the algorithm for two- or three-dimensional operating space comes from the exponential dependence of the complexity on the dimensionality  $D$ . Under the probabilistic approach we are using, the complexity of the algorithm does not depend on the population size.

#### A. Numerical Results

To solve numerical optimal control, we are using the sample time  $\Delta T = 0.03h$ . The terminal time of our problem is  $T = 3h$ . Therefore, the optimal control is approximated by 100 samples. In this example, the control limit is  $u_{\max} = 2$ , and the velocities of moving left and right are  $k_1 = 0.5$  and  $k_2 = 0.25$ , respectively. To avoid the singular control problem, we decide to use the parameter  $\varepsilon = 10^{-7}$ . The initial guess for the optimal control is  $\hat{u}^1(k) = [0.5 \ 0.5 \ 0.5]'$   $\forall k$ .

The cost function  $J^\varepsilon$  value iterations are presented in Fig. 2. The cost function converges to the value of 1.3920. The same figure also shows that the difference between  $J^\varepsilon$  and  $J$  is negligible, as it is expected from (18). From this figure, we can conclude that the optimal control  $\hat{u}^*$  is computed after 44 iterations.

The components of the control  $\hat{u}^*$  are given in Fig. 3. The first component  $\hat{u}_1^*$  starts with zero value, then it changes at  $t = 0.21h$  to 2. Before it turns to 0 again, the control  $\hat{u}_3^*$  has already changed from 0 to 2. Thus, between  $t = 1.71h$  and  $t = 1.74h$ ,  $\hat{u}_1^*$  and  $\hat{u}_3^*$  are both 2. This can be understood as an effective slowdown of the velocity of moving

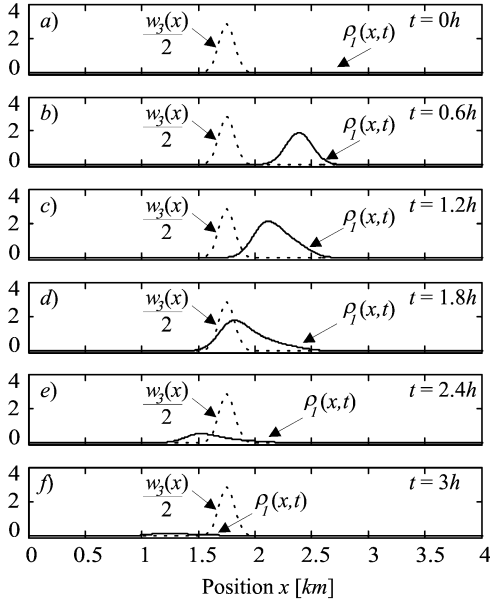


Fig. 4. State PDF evolution of robots moving left  $\rho_1(x,t)$  for  $t = 0.6, 1.2, 1.8, 2.4h$ ,  $u_i \in [0, 2]$ ,  $i = 1, 2, 3$ .

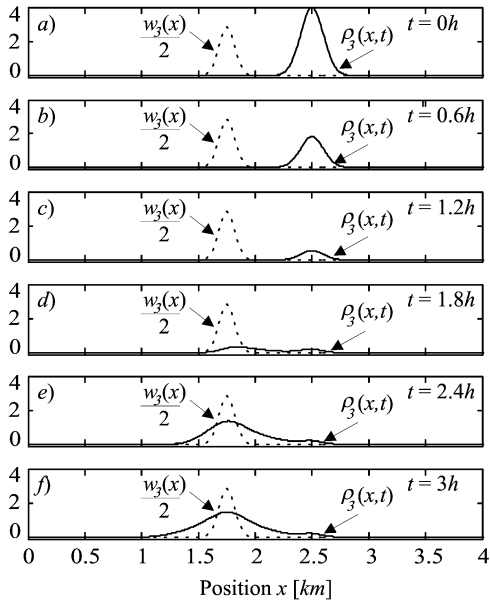


Fig. 5. State PDF evolution of stopped robots  $\rho_3(x,t)$  for  $t = 0.6, 1.2, 1.8, 2.4h$ ,  $u_i \in [0, 2]$ ,  $i = 1, 2, 3$ .

to the left, since each robot makes the transition to *move left* and *stop* states with the highest possible rates. After  $t = 1.74h$ ,  $\hat{u}_1^*$  is 0 and  $\hat{u}_3^*$  is 2 by the end of the time interval  $[0, T]$ . All the time, in this interval,  $\hat{u}_2^*$  is zero, i.e., the optimal control does not include transitions to the discrete state *move right*. Since the initial PDF of robots moving right is  $\rho_2(x, 0) = 0$ , we can conclude that this PDF will be zero all the time, i.e.,  $\rho_2(x, t) = 0 \forall t \in [0, T]$ . Therefore, only the evolutions of  $\rho_1(x, t)$  and  $\rho_3(x, t)$  are presented in Figs. 4 and 5, respectively.

Starting with the initial PDFs  $\rho_i(x, 0)$ ,  $i = 1, 2, 3$ , the control  $\hat{u}^*$  produces distribution evolutions, such that at the terminal time  $T = 3h$ , the PDF  $\rho_3(x, t = T)$ , depicted in Fig. 5, has one peak value at the same position as the  $w_3(x)$  peak. The transition rates are limited, therefore, there are robots that have never moved from the discrete state *stop* at the terminal time  $T$ . This is shown in the plot of  $\rho_3(x, T)$ , where a

small plateau exists for the  $x$  values corresponding to  $\rho_3(x, 0)$  maximum.

We can see from Fig. 5 that our original intuition to produce a sharper robot distribution in the terminal time, in comparison with the distribution in the initial time, has failed. This is because the evolution of  $\rho_3(x, t)$  is constrained by the population dynamics, i.e., the PDE system (1) and the corresponding initial condition (8).

The presented numerical example along with the derivation of this section shows that the minimum principle for PDEs can be exploited for the computation of robotic population optimal control in the same way as Pontryagin's minimum principle is used for ODE optimal-control computation [16], [19].

#### IV. CONCLUSION

In this paper, we introduced the modeling and control approach for a large population of robots controlled by stochastic control signals. It is based on a system of PDEs which describes the evolution of the state PDF of the population. Using this probabilistic description of the population state, we formulated an optimal-control problem, introducing a cost function which includes a weighting function and a state PDF at the terminal time. We showed that the minimum principle for PDEs may be exploited to solve this problem. These results were illustrated using a simulated robotic population.

It is worth mentioning that the state PDF of the population evolves in the same way as the state PDF of one robot with the same initial conditions. Therefore, the same result can be used for modeling and control of one robot in the probabilistic sense.

In this paper, we only considered centralized control, and have designed the best controller applying this strategy. Though the centralized nature of the controller has its well-known drawbacks, it is used here as a means of providing control principles for large-size robotic populations, prone to mathematical analysis and design from specifications. For further improvement of the control performance, local robot controllers must be taken into account. We argue that the best control strategy would be based on a two-level controller. The upper level would be a centralized controller based on the PDE model of the population. It would ensure the coherent behavior of the population by broadcasting commands or settings for the robot control loops. The lower level would be based on local robot controllers, to ensure performance robustness. As future work, we are considering designing such a controller under the framework introduced in this paper. We are also considering extending the application of the PDE minimum principle to other types of optimal criteria, e.g., optimal control with infinite terminal time and different cost functions which can control the shape of the state PDF.

The study of robotic populations by using the approach presented in this paper is of potential interest for the mission control of nanorobots or molecular devices, and applications to smart materials and advanced medical treatments.

#### ACKNOWLEDGMENT

The authors would like to thank Prof. M. Athans for all his useful suggestions. Thanks also to Profs. F. Troltzsch, S. Mitter, and D. Gomes for helpful advice. They are especially thankful to Dr. J. Carneiro for his role in the development of the original modeling framework for biological applications, and Prof. R. de Boer for all the support he gave to this work.

#### REFERENCES

- [1] J. Ferber, *Multi-Agent Systems: An Introduction to Distributed Artificial Intelligence*. Reading, MA: Addison-Wesley, 1999.
- [2] M. Wooldridge, *Introduction to MultiAgent Systems*. New York: Wiley, 2002.

- [3] T. Balch and L. Parker, Eds., *Robot Teams: From Diversity to Polymorphism*. Natick, MA: A. K. Peters, 2002.
- [4] R. Arkin, *Behavior-Based Robotics*. Cambridge, MA: MIT Press, 1998.
- [5] A. Jadbabaie, J. Lin, and A. S. Morse, "Coordination of groups of mobile autonomous agents using nearest neighbor rules," *IEEE Trans. Autom. Control*, vol. 48, no. 6, pp. 988–1001, Jun. 2003.
- [6] H. G. Tanner, G. J. Pappas, and V. Kumar, "Leader-to-formation stability," *IEEE Trans. Robot. Autom.*, vol. 20, no. 3, pp. 443–455, Jun. 2004.
- [7] K. Sugawara and M. Sano, "Cooperative acceleration of task performance: Foraging behavior of interacting multi-robot system," *Physica D*, vol. 100, pp. 343–354, 1997.
- [8] K. Lerman and A. Galstyan, "Mathematical model of foraging in a group of robots: Effect of interference," *Auton. Robots*, vol. 13, pp. 127–141, 2002.
- [9] A. Martinoli, K. Easton, and W. Agassounon, "Modeling swarm robotic systems: A case study in collaborative distributed manipulation," *Int. J. Robot. Res.*, vol. 23, no. 4, pp. 415–436, 2004.
- [10] D. Milutinović, "Stochastic model of microagent populations," Ph.D. dissertation, Inst. Syst. Robot., Inst. Superior Tecnico, Lisbon, Portugal, 2004.
- [11] A. Perelson and G. Weisbuch, "Immunology for physicists," *Rev. Modern Phys.*, vol. 69, no. 4, pp. 1219–1267, Oct. 1997.
- [12] D. Milutinović, P. Lima, and M. Athans, "Biologically inspired stochastic hybrid control of multi-robot systems," in *Proc. 11th Int. Conf. Adv. Robot.*, Coimbra, Portugal, 2003, pp. 708–713.
- [13] H. Jianghai, J. Lygeros, and S. Sastry, *Towards a Theory of Stochastic Hybrid Systems, HSCC 2000*. New York: Springer-Verlag, 2000, pp. 160–173.
- [14] L. D. Landau and E. M. Lifshitz, *Statistical Physics*. New York: Pergamon, 1959.
- [15] H. O. Fattorini, *Infinite Dimensional Optimization and Control Theory*. Cambridge, U.K.: Cambridge Univ. Press, 1999.
- [16] M. Athans and P. L. Falb, *Optimal Control: An Introduction to the Theory and its Applications*. New York: McGraw-Hill, 1966.
- [17] L. C. Evans, *Partial Differential Equations*. Providence, RI: Amer. Math. Soc., 1998.
- [18] D. P. Bertsekas, *Nonlinear Programming*. Belmont, MA: Athena Scientific, 1999.
- [19] O. von Stryk and R. Bulirsch, "Direct and indirect methods for trajectory optimization," *Ann. Oper. Res.*, no. 37, pp. 357–373, 1992.

## Kinematic Control of Platoons of Autonomous Vehicles

Gianluca Antonelli and Stefano Chiaverini

**Abstract**—In this paper, an approach to control the motion of a platoon of autonomous vehicles is presented. The proposed technique is based on the definition of suitable task functions that are handled in the framework of singularity-robust task-priority inverse kinematics. The algorithm is implemented by a two-stage control architecture such that intervehicle communication is not required. The effectiveness of the approach is investigated by means of numerical simulation case studies.

**Index Terms**—Closed-loop inverse kinematics, formation control, multi-robot systems, platoon of vehicles.

### I. INTRODUCTION

A challenging research field for control application is represented by autonomous multirobot systems that exhibit a form of cooperative behavior.

The topic of multirobot systems is so wide, see, e.g., [9] for an overview, that also the terminology is varied: the terms platoon, multirobot, team, formation, group, are frequently used with overlap of meaning. In the remainder, for sake of simplicity, all the above terms will be used as synonyms with a small preference for the term *platoon*. According to the nomenclature in [9], this paper focuses on the problem of *traffic control*, i.e., the path planning of multiple agents/robots/vehicles in a common environment.

Different mathematical approaches have been investigated for this control problem, such as flatness-based theory in [17], aimed at artificially coupling motion of the vehicles, or the use of control graphs in [12], to address the problem of changing the platoon formation. Few studies have also considered from a theoretical point of view the problem of team coordination with underactuated/nonholonomic vehicles [13], [21].

The avoidance of obstacles is, obviously, of primary importance, since most of the platoon's applications concern unstructured environments. The simplest approach is obtained by treating the formation as a single rigid body and applying obstacle avoidance techniques for a single vehicle, such as in [5]. More flexible approaches have been discussed, e.g., in [4], [6], [7], [16], and [19].

Following our previous work in [1] and [2], in this paper, an approach to kinematic control of the shape of a platoon of autonomous vehicles is developed. The proposed technique inherits from the work in [7] the use of suitably defined task functions and the lack of intervehicle communication. Nevertheless, our work handles redundancy resolution in the framework of singularity-robust task-priority inverse kinematics [11], thus overcoming some drawbacks that might be experienced by applying the algorithms described in [7]; the main consequences of this different choice are pointed out in Section III. The control scheme is implemented by a two-stage architecture which only exchanges position reference data from the centralized platoon-formation control algorithm to the single-vehicle motion controllers; obstacle avoidance

Manuscript received February 8, 2006; revised May 4, 2006. This paper was recommended for publication by Associate Editor B. J. Yi and Editor L. Parker upon evaluation of the reviewers' comments. Color versions of Figs. 2 and 3 are available at <http://ieeexplore.org>.

The authors are with the Dipartimento di Automazione, Elettromagnetismo, Ingegneria dell'Informazione e Matematica Industriale (DAEIMI), Università degli Studi di Cassino, 03043 Cassino (FR), Italy (e-mail: antonelli@unicas.it; chiaverini@unicas.it).

Digital Object Identifier 10.1109/TRO.2006.886272